Spontaneous fine-tuning to environment in many-species chemical reaction networks

Jordan M. Horowitz[a,1] and Jeremy L. England[a,1,2]

[a]Physics of Living Systems Group, Department of Physics, Massachusetts Institute of Technology, Cambridge, MA 02139

Edited by Stanislas Leibler, The Rockefeller University, New York, NY, and approved June 12, 2017 (received for review January 12, 2017)

A chemical mixture that continually absorbs work from its environment may exhibit steady-state chemical concentrations that deviate from their equilibrium values. Such behavior is particularly interesting in a scenario where the environmental work sources are relatively difficult to access, so that only the proper orchestration of many distinct catalytic actors can power the dissipative flux required to maintain a stable, far-from-equilibrium steady state. In this article, we study the dynamics of an in silico chemical network with random connectivity in an environment that makes strong thermodynamic forcing available only to rare combinations of chemical concentrations. We find that the long-time dynamics of such systems are biased toward states that exhibit a fine-tuned extremization of environmental forcing.

nonequilibrium thermodynamics | adaptation | chemical reaction networks | self-organization | energy seeking

An arrangement of matter may be said to be finely tuned to its environment if it is configured to interact with that environment in a way that is highly atypical for random rearrangements of its components. Whereas some of the most striking examples of such matching between system and environment are found in the architecture of living things (1, 2), the category is in principle far broader, and one might therefore hope to provide an account of emergent fine-tuning in general physical terms.

Recent progress in theoretical nonequilibrium statistical mechanics (3–7) has helped to clarify a general relationship between the likelihood of a system adopting a particular microscopic configuration and the amount of energy absorbed and dissipated during the system's dynamical history. Essentially, the irreversibility of being driven into a kinetically stable state must be compensated by the release of heat in the surroundings, which frequently occurs when the system absorbs and dissipates energy from an environmental source of work. The implications of this thermodynamic frame are particularly clear in systems where the specific configuration adopted has a large influence on the accessibility of energy from external drives, such that strongly driven states are rare. In such a scenario, having a highly dissipative history becomes tantamount to having a configurational history that includes the rare, finely tuned states that make dissipation possible. This observation suggests that there may be a broad class of nonequilibrium systems for which state-dependent drive strength is the relevant thermodynamic parameter for describing the bias in their exploration of configuration space.

Motivated by these considerations, we carried out simulations of a complexly driven, randomly wired, many-species chemical reaction network, with the aim of identifying a thermodynamic principle governing self-organization far from equilibrium. We found that such networks have a pronounced bias toward settling into rare states in chemical space with extremal forcing, suggesting that emergent fine-tuning is a general tendency of their dynamical behavior.

Two-Species Model

In this study, we are ultimately interested in the thermodynamic properties of the nonequilibrium fixed points that emerge when a many-species chemical system is driven in a way that varies complexly as a function of the system state. However, to illustrate the relationship between dynamics and thermodynamics in a simple example, we first consider a chemical network with only two possible species A and B (with concentrations denoted by the same symbols) that interconvert with rate constants $k_{A\to B} = k_{B\to A}$. In the absence of driving, this network's unique dynamical fixed point is the chemical equilibrium in which $A^* = B^*$. We wish to analyze how an external drive may stabilize new fixed points away from equilibrium. Thus, we now imagine coupling this system to an external source of chemical driving by allowing the same reaction to also proceed via a new pathway with rates $k'_{A\to B}\exp[\mathcal{F}(A,B)] = k'_{B\to A}$ (Fig. 1*A*). The introduction of this new reaction branch may seem surprising at first, but it is quite natural. It simply reflects that there was always another reaction $A \overset{D}{\rightleftharpoons} B$ that could have happened in principle as the result of a catalyst D in the environment, except that it was negligibly slow due to lack of D.

The fact that there is a force $\mathcal{F}(A,B) = \ln(k'_{B\to A}/k'_{A\to B})$ breaks the time-reversal symmetry that was present in the original equilibrium network. Accordingly, the traversal of this new forced reaction branch must involve free-energy dissipation $\mathcal{F}$ in the surroundings (8–10). This could be achieved, for example, if the catalyst D were ATP and converted into ADP and P_i when $A \to B$. In this case, a nontrivial dependence of $\mathcal{F}$ on the chemical concentrations would implicitly be the result of feedback through other chemical actors not represented explicitly in the model: Perhaps B controls a metabolic pathway that affects the ATP concentration. Accordingly, as A and B evolve, the chemical potential drop from ATP to ADP might change, thereby altering the forcing.

Significance

A qualitatively more diverse range of possible behaviors emerge in many-particle systems once external drives are allowed to push the system far from equilibrium; nonetheless, general thermodynamic principles governing nonequilibrium pattern formation and self-assembly have remained elusive, despite intense interest from researchers across disciplines. Here, we use the example of a randomly wired driven chemical reaction network to identify a key thermodynamic feature of a complex, driven system that characterizes the "specialness" of its dynamical attractor behavior. We show that the network's fixed points are biased toward the extremization of external forcing, causing them to become kinetically stabilized in rare corners of chemical space that are either atypically weakly or strongly coupled to external environmental drives.

Author contributions: J.M.H. and J.L.E. designed research, performed research, and wrote the paper.

The authors declare no conflict of interest.

This article is a PNAS Direct Submission.

Freely available online through the PNAS open access option.

[1]J.M.H. and J.L.E. contributed equally to this work.

[2]To whom correspondence should be addressed. Email: jengland@mit.edu.

This article contains supporting information online at www.pnas.org/lookup/suppl/doi:10.1073/pnas.1700617114/-/DCSupplemental.

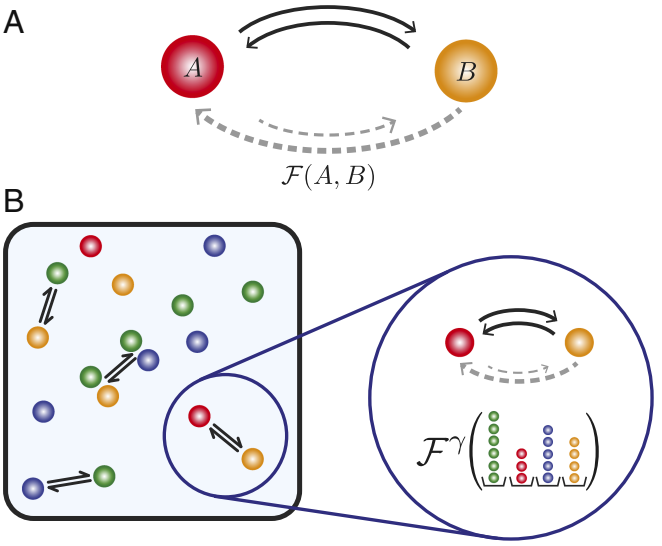

Fig. 1. Illustration of reaction scheme. (*A*) Two species *A* and *B* interconvert through two reactions, one of which (gray) is driven by a state-dependent thermodynamic force $\mathcal{F}(A, B)$. (*B*) A dilute, well-stirred mixture of chemical species (colored circles) interconverts through a random set of reactions. Some reactions are copied and biased by a collection of thermodynamic forces $\mathcal{F}^\gamma$(**A**), which are nonlinear functions of the species' concentration profile.

The rate of dissipation in a fixed point stabilized by such driving would be positive, and the amount of dissipation per reaction would be determined by the chemical potential drop powering the driven reaction. However, the detailed question of whether such a nonequilibrium fixed point might lie at high or low chemical forcing would entirely depend on the assumption of how $\mathcal{F}$ depends on A and B. For example, if $\mathcal{F} = fA$ with $f \gg 1$, then we would expect to see strong positive feedback, whereby a high-force fixed point would be stabilized at $(A^*, B^*) = (A_{\max}, 0)$. In the following, we consider systems in which $\mathcal{F}$ varies ruggedly over a multidimensional chemical space, so that the emergent fixed points are no longer obvious.

Many-Species Model

We set out to study the dynamics of a randomly wired chemical network of many reacting species in a dilute, well-stirred mixture, driven out of equilibrium by complexly structured thermodynamic forces induced by the surroundings, schematically illustrated in Fig. 1*B*.

As detailed in *Materials and Methods*, species were allowed to participate in one-body, two-body, and catalyzed three-body reaction channels ($A \rightleftharpoons B$, $A + B \rightleftharpoons C + D$, and $A + B + E \rightleftharpoons C + D + E$) with mass-action kinetics (11). No reactions were allowed that amounted to direct self-replication of any one species (e.g., $A + B \rightleftharpoons A + A$), to avoid classic mechanisms of selection (12). Undriven rate constants for the reactions were randomly chosen from a distribution that comprised multiple timescales, with the fastest being 1 s to set the units of time. Each species was assumed to have the same equilibrium free energy.

Thus described, such a chemical reaction network has a single dynamical fixed point (known as its chemical equilibrium point) where the concentrations of all different species are equal. To drive the system away from equilibrium, we introduce a collection of additional reaction channels biased by various thermodynamic forces $\mathcal{F}^\gamma$. The key here is our choice of external forcing, in other words, how we model the effect of the environment on the system. In a fully detailed description, an explicit model of every possible reaction within both the system and the surroundings would be necessary to predict the dynamics. Our goal here is to strip away most of this detail and focus on the essential physical characteristics of the environment's effect on the system. In particular, we aim to explore the general physical consequences of a circumstance in which the "fuel" in the surroundings may be exploited only when the chemical concentrations arrange themselves into exceptional configurations. We call such conditions "challenging" because they implicitly define a physical criterion that most possible configurations of the system fail to satisfy and thus provide an ideal setting in which to search for fine-tuning to environmental energy sources; put another way, the rarity of high (or low)-force arrangements makes their appearance exceptional and therefore recognizable.

To this end, we chose forcing functions $\mathcal{F}^\gamma$ that were generated as random functions of concentration following a mathematical form known to lead to many-bodied frustration (13, 14), so that concentration profiles for which the strength of forcing was extremely high or low were much more difficult to realize than combinations for which forcing was mediocre (Fig. 2*C*) (*Materials and Methods*). Note that whereas the forcing function itself contains no explicit time dependence, it does depend strongly on the system state. To achieve this manner of forcing in an explicit model would in general require a complex collection of hidden degrees of freedom that more rapidly relax to a nonequilibrium steady state determined both by the system state and by the fixed chemical potentials of various external particle baths. However, because of the fundamental relationships that hold between kinetic and thermodynamic quantities, a consistent picture of the thermodynamic fluxes flowing through these hidden processes can be inferred from the system kinetics alone.

We implemented this forcing scheme on a many-species chemical reaction network by randomly selecting a subset of reaction channels for duplication and asymmetrization. Thus, for a given channel $A \rightleftharpoons B$ with undriven rate constants $k_{A\to B} = k_{B\to A} = k$, we create a second, new, time-asymmetric version with rate constants $k'_{A\to B} = k'\ e^{\mathcal{F}^\gamma/2}$ and $k'_{B\to A} = k'\ e^{-\mathcal{F}^\gamma/2}$. Such a description will always be thermodynamically consistent as long as we recognize that the forcing, which breaks detailed balance, measures the (minimum) amount of free energy dissipation in the environment consistent with the amount of asymmetrization

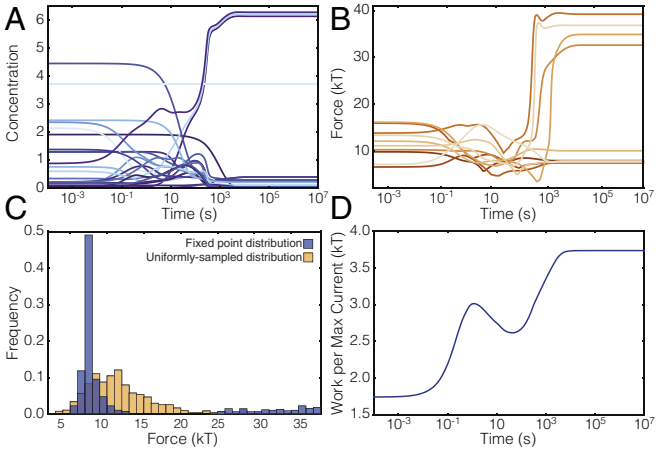

Fig. 2. Thermodynamic characterization of a reaction network. (*A*) Single representative dynamical trajectory of the 25 chemical species' concentrations. (*B*) Time evolution of the total thermodynamic force magnitude $\mathcal{F}_{\text{tot}}$ for 10 different initial conditions. (*C*) Normalized histogram of the total force $\mathcal{F}_{\text{tot}}$ from 1,000 uniform samples of configuration space (orange) compared with the normalized histogram of the total force $\mathcal{F}_{\text{tot}}$ attained after 10^7 s for 500 trajectories with uniform initial conditions (blue). (*D*) Work per maximum current $\eta = \sum_i J_i \mathcal{F}^{\gamma i} / \max_i |J_i|$, which measures the relative contribution of each reaction channel to the total flux, as a function of time for the trajectory in *A*.

in the rates (15). Thus, we can consistently discuss the energetics and thermodynamics of the system without having to specifically model the surroundings. Indeed, explicitly denoting the net number of reactions through a driven reaction channel as J, the dissipation takes the familiar flux times force form $J\mathcal{F}^{\gamma}$. It should also be noted that in our initial investigation, we assumed $k' = k$, reasoning that shared transition-state properties could cause these rates to be strongly correlated. As we shall see below, however, it is possible to relax this assumption without altering the effect we observe.

Let us summarize that the motivation for our choice of the $\mathcal{F}^{\gamma}$s was to ensure that the chemical space contains a few, rare states that exhibit a fine-tuned matching to an environmental drive. It must be emphasized, however, that there is no obvious reason at the outset to expect the system should tend to find or stay in these rare, finely tuned states—unlike in the obvious case of the one-reaction model above, the complexity of dynamics exceeds our ability to intuit which parts of chemical space will prove to be kinetically stable. A priori the high-force regions are simply locations in concentration space that experience strong irreversibility in their reactive flux when the system happens to visit them over the course of its dynamical evolution, and it is the empirical question investigated below whether their thermodynamic specialness requires that they turn out to be something more as well.

Results

With the reactions fixed, the dynamical evolution of the $N = 25$ chemical species $\mathbf{A} = \{A_1, \ldots, A_{25}\}$ is given by the nonlinear, deterministic reaction rate equations $\dot{\mathbf{A}} = \mathbf{Z}(\mathbf{A})$, where the vector field $\mathbf{Z}$ is constructed using mass-action kinetics. We numerically solved the reaction rate equations for many randomly generated chemical reaction networks, choosing initial conditions uniformly from the simplex of species concentrations with total $C = \sum_i A_i$ fixed to 25 (on average 1 mol/vol of each species). A number of parameters had to be chosen before a given family of random reaction networks could be realized and simulated. Details of all these calculations are described in *Materials and Methods*. We did not carry out a systematic search of parameter space, which is far too vast, but we found in general that the effects reported below required that nonequilibrium forcing be sufficiently strong, the number of catalyzed reactions be sufficiently large, and reaction graph connectivity be sufficiently sparse. Other than these qualitative constraints, the phenomena observed arose generically across the range of parameter values we examined.

In general, the dynamics evolved to one of many possible fixed points [i.e., to one of the solutions $\mathbf{A}^*$ of $\mathbf{Z}(\mathbf{A}^*) = 0$], depending on the initial conditions. The results for a representative example of a reaction network are displayed in Fig. 2.

Fig. 2*A* shows the concentration dynamics of the 25 species. The most striking feature of this realization is that, on a timescale $\sim 10^3$ s (which corresponds to the rate of the slowest unforced reactions) a significant change in the concentration profile occurs: Three species precipitously grow in mass fraction together while all others drop in concentration. Other realizations instead would relax into a configuration where all of the species have roughly equal, small concentrations (Fig. S1).

We designed the chemical space of this system to contain rare states of extremal thermodynamic forcing, which might be recognized as examples of apparent fine-tuning. Thus, we undertook to analyze the total force magnitude on the network over the course of its dynamical evolution. Labeling the force on the ith reaction as $\mathcal{F}^{\gamma_i}$, we computed this quantity for the network as

$$\mathcal{F}_{\text{tot}} = \sum_i |\mathcal{F}^{\gamma_i}|. \qquad [1]$$

This sum can be large either because a few reactions are strongly forced or because many reactions are moderately forced; in any case, it acts as a simple measure of whether the network as a whole is experiencing strong driving.

In the particular realization in Fig. 2*B*, we see the forcing tended to exhibit one of two behaviors. In one scenario, forcing stayed low or decreased; these outcomes corresponded to final concentration distributions that were relatively close to uniform, indicating a near-equilibrium behavior. Alternatively, it was also often the case that the forcing would rise to an extremely high value as the system approached a fixed point.

This observation is made precise in Fig. 2*C* by comparing a histogram of total forces obtained from a uniform sampling of chemical space with the histogram of the final total force at the end of the trajectories, where the dynamics have reached a fixed point. The motivation for this comparison is to detect whether the dynamical fixed points appear to be exceptional combinations of their constituents compared with the ensemble of random rearrangements achieved through uniform sampling of chemical space.

The final force distribution for the representative network studied in Fig. 2 displays a bimodal structure, with the final total forces being either exceptionally high or low, relative to the uniformly sampled set. Whereas other network realizations did not necessarily show this bimodal structure, their final total force distributions were peaked at either unusually high or low levels, essentially filling in one or the other of the humps of the bimodal distribution (Fig. S1). Thus, the dynamical evolution appeared to be biased toward landing on fixed points that have recognizably special and atypical thermodynamic relationships to their external environment (16).

To test for this bias more rigorously, we randomly realized 200 different reaction networks with distinct connectivity, unforced reaction timescales, and forcing parameters and then evolved their dynamics from five random initial conditions. To assess the atypicality of the final total force $\mathcal{F}_{\text{tot}}$ reached at the dynamical fixed point for each trajectory, we computed how likely the observed $\mathcal{F}_{\text{tot}}$ would have been in the same network if it had been sampled from a uniform distribution over concentration space. We did so by generating the uniformly sampled forcing distribution as in Fig. 2*C* for each randomly realized network and then assigning a percentile rank in this distribution for each fixed point reached. For example, a trajectory ending with final total force $\mathcal{F}^*$ assigned a percentile rank of 80 means that 80% of the values of $\mathcal{F}_{\text{tot}}$ observed from uniform sampling over configuration space were less than $\mathcal{F}^*$. Final total forces exceeding the largest uniformly sampled $\mathcal{F}_{\text{tot}}$ were assigned a percentile rank of 100+, representing extremely large forcing.

As a further control, we uniformly sampled configuration space a second time and determined the percentile rank of the observed total force according to the same procedure by which the fixed points were ranked; Fig. 3*A*, *Inset* is a histogram of these percentile ranks for fixed points and for the control set. By computing the ratio between these two histograms we quantified the bias toward each percentile rank, which is displayed in Fig. 3*A*.

Strikingly, the final force percentile distribution separates into two types of behavior, paralleling the outcomes observed in the single reaction network studied above. Frequently, the fixed point of a random reaction network resides at low force, corresponding to a near-equilibrium fine-tuned outcome: The system gets stuck in a near-equilibrium state that is atypically decoupled from the external drive. However, there is also a heavy tail in the percentile distribution, and a significant fraction of all trajectories terminate at fixed points with percentile ranks above 100, with a likelihood that is four times that of the control; these realizations correspond to arrangements in which the system discovers a way of harvesting energy from the atypically strong

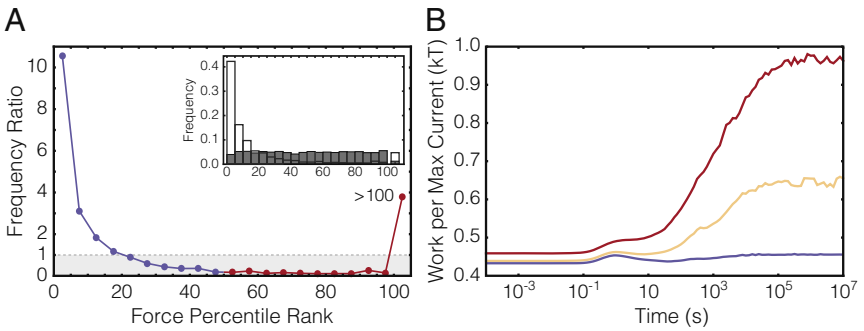

Fig. 3. Characterization of final total forcing $\mathcal{F}_{\text{tot}}$ rarity. (*A*) Frequency ratio of the percentile ranks of final total forces $\mathcal{F}_{\text{tot}}$ to percentile ranks of uniformly sampled control measured relative to a uniformly sampled distribution of forces over configuration space. Shading delimits the region where the final total force $\mathcal{F}_{\text{tot}}$ occurs less often than the control. (*A*, *Inset*) Normalized histogram of final total force $\mathcal{F}_{\text{tot}}$ percentile (white) and control (gray). (*B*) Work per maximum current η as a function of time, averaged over all reaction networks (yellow) and conditioned on ending in a high-forced fixed point (red) or a low-force fixed point (blue).

forcing, thereby maintaining itself in a recognizably special out-of-equilibrium arrangement.

We also computed the work rate per maximum current, $\eta = \sum_i J_i \mathcal{F}^{\gamma_i} / \max_i |J_i|$, which measures the dissipation per reaction, weighted to favor those reactions experiencing the most current. Averaged over many realizations, the mean value of η is seen to increase dramatically over time in Fig. 3*B*, despite the greater frequency of low-force fixed points. In aggregate, the high-force fixed points thus lead to such a pronounced increase in η that they dominate the mean. Increased effectiveness of work absorption from external drives therefore appears to be a robust average feature of a large random ensemble of reaction schemes.

Our observations lead us to ask how the dynamics of these random networks become biased toward having fixed points that are thermodynamically special. What is it about these rare configurations—which make up a minuscule fraction of the whole chemical space—that causes them so frequently to turn out to be the inevitable dynamical attractor?

To explain this, we note that in our model, all driven reactions were duplicated from an existing undriven version. Accordingly, we can divide the equations of motion into undriven and driven pieces, $\dot{\mathbf{A}} = \mathbf{Z}_{\text{driven}}(\mathbf{A}) + \mathbf{Z}_{\text{undriven}}(\mathbf{A})$. From this division, it is immediately clear that any dynamical fixed point $\mathbf{A}^*$ must satisfy $\mathbf{Z}_{\text{driven}}(\mathbf{A}^*) = -\mathbf{Z}_{\text{undriven}}(\mathbf{A}^*)$. It should also be the case, however, that in the limit of no driving $\mathbf{Z}_{\text{driven}}(\mathbf{A}^*)$ will be highly correlated with $\mathbf{Z}_{\text{undriven}}(\mathbf{A}^*)$, because they have many identical rate equation terms in common. [Indeed, if all reaction channels are duplicated and forcing is taken to zero, $\mathbf{Z}_{\text{driven}}(\mathbf{A}^*) = \mathbf{Z}_{\text{undriven}}(\mathbf{A}^*)$]. Thus, any nontrivial high-force fixed point must occur at a place in configuration space that is sufficiently driven to break the relationship between $\mathbf{Z}_{\text{driven}}$ and $\mathbf{Z}_{\text{undriven}}$, decorrelating them enough so that they could happen to additively cancel.

To assess the impact of high forcing, we investigated how it shifts the Pearson correlation (or normalized inner product) ρ between $\mathbf{Z}_{\text{driven}}$ and $\mathbf{Z}_{\text{undriven}}$. The Pearson correlation is a bounded $(-1 < \rho < 1)$ measure of correlation. Positive values near $\rho \approx 1$ signify $\mathbf{Z}_{\text{driven}}$ and $\mathbf{Z}_{\text{undriven}}$ point roughly in the same direction in chemical space and therefore cannot cancel to produce a fixed point; in contrast, negative values near $\rho \approx -1$ imply $\mathbf{Z}_{\text{driven}}$ and $\mathbf{Z}_{\text{undriven}}$ are pointing in opposite directions, allowing for the possibility of a fixed point. Fig. 4 displays distributions of Pearson correlations conditioned on the total force for $40,000$ configurations obtained from 400 reaction networks.

Low-force configurations have a correlation peaked near $\rho \approx 1$, which is consistent with our intuition that when the total thermodynamic force is low, it cannot reshape the driven reactions so that $\mathbf{Z}_{\text{driven}} \approx -\mathbf{Z}_{\text{undriven}}$. By contrast, high-force configurations have a correlation distribution with a pronounced tail extending to $\rho \approx -1$. Thus, forcing decorrelates the direction of the driven and undriven force fields. Meanwhile, the scatter plot of $\|\mathbf{Z}_{\text{undriven}}\|$ vs. $\|\mathbf{Z}_{\text{driven}}\|$ in Fig. 4*B* demonstrates that the magnitudes of these two reaction vectors remain largely unchanged, and correlated, even at high force. With these two different vectors sampled quasi-independently, there is an increased likelihood that they will turn out to be equal and opposite, canceling out to a high-force fixed point. The key to this mechanism is the high dimensionality of the chemical space and the random strength and direction of forcing on reactions.

Discussion

In the ensemble of random reaction networks studied here, a challenging driving environment made it possible to define fine-tuned order in terms of an atypically strong matching to available sources of work. As anticipated in previous theoretical works (7, 17), our central finding was that kinetically stable behaviors of such a system are indeed biased toward appearing to be finely tuned to the external drive: In other words, the long-time behavior of the system is enriched in outcomes that would be observed only with small likelihood in a random and uniform sampling of the whole space of possibilities.

The mechanism for emergent fine-tuning at high force appears to require that randomly interacting components lead to a high-dimensional space of possible configurations with distinct properties. To maintain a high-force fixed point, the system must experience enough forcing from the environment to give rise to driven reactive fluxes that can exactly counterbalance the undriven reactions occurring alongside them. Whereas such counterbalancing is by no means guaranteed to occur solely as the result of high forcing, the high-force regime is composed of different locations in chemical space that may be thought of as each being a quasi-independent attempt at achieving this counterbalancing by random accident. In a setting where the effective number of such attempts is large enough, the existence of at least one high-force fixed point can be surprisingly likely.

We might have suspected that our initial assumption that forced and unforced reaction branches were governed by the same reaction timescales ($k = k'$) was an important ingredient; it stands to reason that the correlation of timescale increases the degree to which the driven and undriven reaction vectors must point in the same direction. However, when we regenerated the same plots in Figs. 3 and 4 using reaction networks in which k and k' were independently drawn (Figs. S2 and S3), we obtained nearly identical results. This robustness derives from the fact that the correlation in direction of driven and undriven

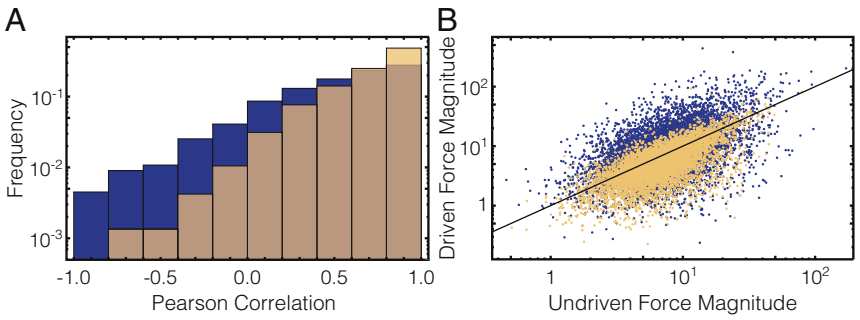

Fig. 4. Characterization of driven and undriven dynamics. (*A*) Normalized histogram of Pearson correlation between driven and undriven force fields, $\mathbf{Z}_{\text{driven}}$ and $\mathbf{Z}_{\text{undriven}}$, for low-force configurations (orange) and high-force configurations (blue). (*B*) Scatter plot of the magnitude of the undriven force field $\|\mathbf{Z}_{\text{undriven}}\|$ vs. the driven force field $\|\mathbf{Z}_{\text{driven}}\|$ conditioned on low-force configurations (orange) and high-force configurations (blue).

reaction vectors at low forcing comes about from factors other than the reaction-by-reaction matching of timescales, which suggests the effect we observe may be general to a larger class of nonequilibrium chemical networks.

We found in general that, once such an attractive fixed point exists, the system dynamics can find it on the timescale of the slowest unforced reaction. At first, this rate of relaxation to the steady state may seem unexpectedly rapid: A structure of correlations in concentration extending across the entire system turns out not to take significantly longer to develop than the time for a single slow reaction to occur at random. The reason for this effect is that we have modeled this chemical network using mass-action kinetics, which assume a limit of large particle numbers. Thus, implicitly, the system has the opportunity to "experiment" with many different chemical combinations in parallel at the level of individual stochastic molecular events, until a successfully cooperative one is discovered (18, 19).

It is instructive to be able to demonstrate that even a chemical mixture devoid of any obvious selective pressure via self-replication could discover and stay in specially structured combinations that appear to be good at meeting a complex challenge presented by the environment—they can not only do this, but also do so on timescales rapid enough to be accessible to direct observation. With further study, such knowledge might prove to be useful in explaining or promoting the emergence of life-like behaviors in initially lifeless material settings.

Materials and Methods

Our model is a well-stirred, dilute mixture of $N = 25$ chemically reacting species, $\mathbf{A} = \{A_1, \cdots A_{25}\}$, with equal free energies in a solute of volume $V = 1$ at inverse temperature $\beta = 1/k_B T$. The species are "wired" together into a chemical reaction network by randomly choosing pairs of species to interconvert through one of $\alpha = 1, \ldots, M$ reversible, chemical reaction channels,

$$\sum_j r_j^\alpha A_j \rightleftharpoons \sum_k s_k^\alpha A_k, \qquad [2]$$

with $r_j^\alpha \in \{0, 1\}$ and $s_k^\alpha \in \{0, 1\}$. Most reactions are unimolecular—there is only one reactant and one product—although with probability $p = 0.3$, a reaction is designed to be bimolecular—two reactants and products. In addition, with probability $e = 0.5$ a catalyst is added to both sides of the reaction (as a reactant and product, so it is not consumed), which is uniformly chosen as a distinct chemical species. This avoids any self-replication reactions.

The reaction rates are given by mass-action kinetics (11),

$$R_+^\alpha(\mathbf{A}) = k^\alpha \prod_j A_j^{r_j^\alpha} \qquad R_-^\alpha(\mathbf{A}) = k^\alpha \prod_j A_j^{s_j^\alpha}, \qquad [3]$$

where $\pm$ denotes the forward and reverse reaction, and the bare rate constants $\{k^\alpha\}$ are chosen at random from the set $\{1\,\text{s}, 10^{-1}\,\text{s}, 10^{-2}\,\text{s}, 10^{-3}\,\text{s}\}$. The bare rates $\{k^\alpha\}$ must be symmetric between the forward and reverse reactions to comply with detailed balance, as the free energies of each species are equal and no species appears more than once as a reactant or product.

We break detailed balance by introducing additional biased reactions driven by a collection of nonlinear, generalized thermodynamic forces. To this end, we randomly select a fraction $\delta = M_{\text{driven}}/M$ of reactions and copy (or clone) them. However, the forward reaction is sped up and the reverse reaction is slowed down by tilting the reaction rate with one of $\gamma = 1, \ldots, f$ thermodynamic forces. The forces are constructed as the bilinear sums

$$\mathcal{F}^\gamma(\mathbf{A}) = \sum_{i>j} J_{ij}^\gamma (A_i - c_i^\gamma)(A_j - c_j^\gamma). \qquad [4]$$

For each force γ, a fixed fraction μ of the coupling constants J_{ij}^γ are nonzero with a magnitude chosen uniformly from the range $(-s, s)$. The offsets c_i^γ are randomly selected to be either 0 or 1. This form for the forcing was chosen because it is well known to be a "frustrated" function of all of the variables A_i whose extremal value is rare (13, 14). The forced reaction kinetics are then

$$\mathcal{R}_+^\alpha(\mathbf{A}) = e^{\beta \mathcal{F}^{\gamma_\alpha}(\mathbf{A})/2} R_+^\alpha(\mathbf{A}), \quad \mathcal{R}_-^\alpha(\mathbf{A}) = e^{-\beta \mathcal{F}^{\gamma_\alpha}(\mathbf{A})/2} R_-^\alpha(\mathbf{A}). \qquad [5]$$

Note that by construction every driven reaction has an undriven copy. As a result, no matter how much the forcing slows down the reaction, the undriven path is still possible, meaning that no reaction can be slower than the rate dictated by the slowest unforced rate constant.

With the rates, the species-concentration dynamics are dictated by the macroscopic reaction rate equations

$$\dot{A}_i = \sum_{\alpha=1}^{M} s_i^\alpha R_+^\alpha(\mathbf{A}) - r_i^\alpha R_-^\alpha(\mathbf{A}) + \sum_{\rho=1}^{M_{\text{driven}}} s_i^\rho \mathcal{R}_+^\rho(\mathbf{A}) - r_i^\alpha \mathcal{R}_-^\rho(\mathbf{A}) \qquad [6]$$

$$\equiv Z_{\text{undriven}}^i(\mathbf{A}) + Z_{\text{driven}}^i(\mathbf{A}) \equiv Z_i(\mathbf{A}). \qquad [7]$$

In summary, the random ensemble of networks is specified by the following collection of parameters: (*i*) N, number of chemical species; (*ii*) M, number of reaction channels; (*iii*) p, average fraction of bimolecular reactions; (*iv*) e, average fraction of catalyzed reactions; (*v*) k^α, bare rate constants; (*vi*) δ, fraction of reactions that are duplicated and forced; (*vii*) f, number of generalized thermodynamic forces; (*viii*) μ, fraction of nonzero bilinear coupling constants in the thermodynamic forces; and (*ix*) s, range of possible magnitudes of the thermodynamic forces' coupling constants.

Numerical solutions were obtained using the NDSolve function in Wolfram Mathematica version 10.1.0.0, using the "StiffnessSwitching" method with accuracy goal set to infinity. Parameters were as follows: For Fig. 2, $N = 25$, $M = 35$, $\delta = 0.3$, $f = 10$, $\mu = 0.3$, and $s = 0.2$. For Fig. 3, there was an even mixture of 1,000 realizations from each of the four ensembles of random networks with (*i*) $N = 25$, $M = 35$, $\delta = 0.6$, $f = 10$, $\mu = 0.2$, $s = 0.2$; (*ii*) $N = 25$, $M = 22$, $\delta = 0.3$, $f = 10$, $\mu = 0.3$, $s = 0.2$; (*iii*) $N = 25$, $M = 35$, $\delta = 0.3$, $f = 10$, $\mu = 0.3$, $s = 0.3$; and (*iv*) $N = 25$, $M = 35$, $\delta = 0.6$, $f = 2$, $\mu = 0.2$, $s = 0.2$. And for Fig. 4, $N = 25$, $M = 35$, $\delta = 0.6$, $f = 10$, $\mu = 0.2$, and $s = 0.2$.

ACKNOWLEDGMENTS. The authors are grateful to Dan Goldman, Pankaj Mehta, and Robert Marsland for thoughtful comments on this article. J.M.H. and J.L.E. are supported by the Gordon and Betty Moore Foundation through Grant GBMF4343. J.L.E. further acknowledges the Cabot family for their generous support of Massachusetts Institute of Technology.

1. Blount ZD, Barrick JE, Davidson CJ, Lenski RE (2012) Genomic analysis of a key innovation in an experimental Escherichia coli population. *Nature* 489:513–518.
2. Milo R, et al. (2002) Network motifs: Simple building blocks of complex networks. *Science* 298:824–827.
3. Crooks GE (1999) Entropy production fluctuation theorem and the nonequilibrium work relation for free energy differences. *Phys Rev E Stat Phys Plasmas Fluids Relat Interdiscip Topics* 60:2721–2726.
4. Seifert U (2008) Stochastic thermodynamics: Principles and perspectives. *Eur Phys J B* 64:423–431.
5. Jarzynski C (2011) Equalities and inequalities: Irreversibility and the second law of thermodynamics at the nanoscale. *Annu Rev Condens Matter Phys* 2:329–351.
6. England JL (2013) Statistical physics of self-replication. *J Chem Phys* 139:121923.
7. Perunov P, Marsland RA, England JL (2016) Statistical physics of adaptation. *Phys Rev X* 6:021036.
8. Qian H, Beard DA (2005) Thermodynamics of stoichiometric biochemical networks in living systems far from equilibrium. *Biophys Chem* 114:213–220.
9. Schmiedl T, Seifert U (2007) Stochastic thermodynamics of chemical reaction networks. *J Chem Phys* 126:044101.
10. Poletinni M, Esposito M (2014) Irreversible thermodynamics of open chemical networks. I. Emergent cycles and broken conservation laws. *J Chem Phys* 141:024117.
11. Van Kampen NG (2007) *Stochastic Processes in Physics and Chemistry* (Elsevier, Amsterdam), 3rd Ed.
12. Nowak MA (2006) Five rules for the evolution of cooperation. *Science* 314:1560–1563.
13. Sherrington D, Kirkpatrick S (1975) Solvable model of a spin-glass. *Phys Rev Lett* 35:1792.
14. Derrida B (1980) Random-energy model: Limit of a family of disordered models. *Phys Rev Lett* 45:79–82.
15. Esposito M (2012) Stochastic thermodynamics under coarse graining. *Phys Rev E* 85:041125.
16. Pross A, Khodorkovsky V (2004) Extending the concept of kinetic stability: Toward a paradigm for life. *J Phys Org Chem* 17:312–316.
17. England JL (2015) Dissipative adaptation in driven self-assembly. *Nat Nanotechnol* 10:919–923.
18. Dyson FJ (1982) A model for the origin of life. *J Mol Evol* 18:344–350.
19. Vaidya N, et al. (2012) Spontaneous network formation among cooperative RNA replicators. *Nature* 491:72–77.